SCIENCE CHINA
Physics, Mechanics & Astronomy

• Article •

August 2015 Vol. 58 No. 8: 082001
doi: 10.1007/s11433-015-5667-6

Deformation dependence of symmetry energy coefficients of nuclei

MO QiuHong[1], LIU Min[1], CHENG LiChun[2] & WANG Ning[1*]

[1]*Department of Physics, Guangxi Normal University, Guilin 541004, China;*
[2]*School of Material Science and Engineering, Guilin University of Electronic Technology, Guilin 541004, China*

Received December 24, 2014; accepted February 28, 2015

Based on the semi-classical Thomas-Fermi approximation together with the Skyrme energy-density functional, we study the deformation dependence of symmetry energy coefficients of finite nuclei. The symmetry energy coefficients of nuclei with mass number A = 40, 100, 150, 208 are extracted from two-parameter parabola fitting to the calculated energy per particle. We find that the symmetry energy coefficients decrease with the increase of nuclear quadrupole deformations, which is mainly due to the isospin dependence of the difference between the proton and neutron surface diffuseness. Large deformations of nuclei can cause the change of the symmetry energy coefficient by about 0.5 MeV and the influence of nuclear deformations on the symmetry energy coefficients is more evident for light and intermediate nuclei.

symmetry energy, Skyrme energy-density functional, nuclear deformation, Thomas-Fermi

PACS number(s): 21.65.Ef, 21.10.Dr

Citation: Mo Q H, Liu M, Cheng L C, et al. Deformation dependence of symmetry energy coefficients of nuclei. Sci China-Phys Mech Astron, 2015, 58: 082001, doi: 10.1007/s11433-015-5667-6

1 Introduction

Nuclear symmetry energy has attracted a lot of attention in recent years. In addition to its importance in the study of nuclear physics such as some crucial information on nuclear structure and reactions, the symmetry energy is also closely related to a large number of astrophysical phenomena. For example, the symmetry energy is of great significance for the study of the structure, the evolution mechanism and the mass-radius relationship of neutron stars [1]. Although a great effort has been devoted in recent decades to investigate the symmetry energy [2–14], the density dependence of the symmetry energy, especially at sub-saturation and supersaturation density regions, is far from clear. More investigations on the symmetry energy are still required.

In ref. [15], Liu et al. studied the nuclear symmetry energy at subnormal densities from the measured nuclear masses [16]. The symmetry energy coefficients were extracted from the masses and some evident oscillations in the mass-dependence of the symmetry energy coefficients were observed. When the shell corrections are taken into account, the oscillations in the extracted symmetry energy coefficients are reduced effectively. Because the shell effects in the measured masses are correlated with nuclear deformations, it is therefore interesting to see how large the nuclear deformations individually affect the symmetry energy coefficients due to the surface-symmetry term and the nuclear surface diffuseness, based on theoretical models and removing the influence of the shell effects.

The density functional theory is widely used in the study of the nuclear ground state which provides us with a useful balance between accuracy and computation cost, allowing large systems with a simple self-consistent manner. In the framework of the effective Skyrme interaction [17] and the extended Thomas-Fermi approximation, the Skyrme energy density functional approach was proposed for the study of nuclear structure and reactions [18–20]. One of the advantages in the semi-classical extended Thomas-Fermi approach

*Corresponding author (email: wangning@gxnu.edu.cn)

is that the microscopic shell and pairing corrections can be clearly removed, which is helpful to study the deformation energies without the influence of the shell effects.

In this work, we will study the "macroscopic" energies of nuclei, especially the deformation dependence of the symmetry energy coefficient, based on the extended Thomas-Fermi approximation together with the Skyrme energy-density functional.

2 The Skyrme energy-density functional and the extended thomas-fermi approach

The energy of a nucleus at its ground state can be expressed as the integral of nuclear energy density functional:

$$E = \int \mathcal{H}\, \mathrm{d}\boldsymbol{r}. \tag{1}$$

The energy density functional $\mathcal{H}(\boldsymbol{r})$ contains the Skyrme energy density $\mathcal{H}_{\rm Sky}(\boldsymbol{r})$ and the Coulomb energy density $\mathcal{H}_{\rm Coul}(\boldsymbol{r})$:

$$\mathcal{H}(\boldsymbol{r}) = \mathcal{H}_{\rm Sky}(\boldsymbol{r}) + \mathcal{H}_{\rm Coul}(\boldsymbol{r}). \tag{2}$$

The Skyrme energy density can be expressed in terms of the local nucleon densities $\rho_{\rm q}(\boldsymbol{r})$, kinetic energy densities $\tau_{\rm q}(\boldsymbol{r})$ and spin-orbit densities $\boldsymbol{J}_{\rm q}(\boldsymbol{r})$ ($q = n$ for neutrons and $q = p$ for protons):

$$\begin{aligned}\mathcal{H}_{\rm Sky}(\boldsymbol{r}) =& \frac{\hbar^2}{2m}\tau + \frac{1}{2}t_0\left[\left(1+\frac{1}{2}x_0\right)\rho^2 - \left(x_0+\frac{1}{2}\right)(\rho_n^2+\rho_p^2)\right]\\ &+ \frac{1}{12}t_3\rho^\alpha\left[\left(1+\frac{1}{2}x_3\right)\rho^2 - \left(x_3+\frac{1}{2}\right)(\rho_n^2+\rho_p^2)\right]\\ &+ \frac{1}{4}\left[t_1\left(1+\frac{1}{2}x_1\right) + t_2\left(1+\frac{1}{2}x_2\right)\right]\tau\rho\\ &+ \frac{1}{4}\left[t_2\left(x_2+\frac{1}{2}\right) - t_1\left(x_1+\frac{1}{2}\right)\right](\tau_n\rho_n+\tau_p\rho_p)\\ &+ \frac{1}{16}\left[3t_1\left(1+\frac{1}{2}x_1\right) - t_2\left(1+\frac{1}{2}x_2\right)\right](\nabla\rho)^2\\ &- \frac{1}{16}\left[3t_1\left(x_1+\frac{1}{2}\right) + t_2\left(x_2+\frac{1}{2}\right)\right][(\nabla\rho_n)^2+(\nabla\rho_p)^2]\\ &+ \frac{1}{2}W_0[\boldsymbol{J}\cdot\nabla\rho + \boldsymbol{J}_n\cdot\nabla\rho_n + \boldsymbol{J}_p\cdot\nabla\rho_p],\end{aligned} \tag{3}$$

where t_0, t_1, t_2, t_3, x_0, x_1, x_2, x_3, α are the Skyrme interaction parameters. W_0 denotes the strength of the spin-orbit interaction. In the calculations, we adopt the Skyrme parameter set SkM* [21] and SLy4 [22]. The kinetic energy density $\tau = \tau_p + \tau_n$ and the spin-orbit density $\boldsymbol{J} = \boldsymbol{J}_p + \boldsymbol{J}_n$ are described by using the extended Thomas-Fermi approach up to the second order in $\hbar$ (ETF2) [18–20].

The kinetic energy density is then expressed as:

$$\begin{aligned}\tau_q[\rho_q(\boldsymbol{r})] =& \frac{3}{5}(3\pi^2)^{2/3}\rho_q^{5/3} + \frac{1}{36}\frac{(\nabla\rho_q)^2}{\rho_q}\\ &+ \frac{1}{3}\Delta\rho_q + \frac{1}{6}\frac{\nabla\rho_q\nabla f_q + \rho_q\Delta f_q}{f_q}\\ &- \frac{1}{12}\rho_q\left(\frac{\nabla f_q}{f_q}\right)^2 + \frac{1}{2}\rho_q\left[\frac{2m}{\hbar^2}\frac{W_0}{2}\frac{\nabla(\rho+\rho_q)}{f_q}\right]^2\end{aligned} \tag{4}$$

with the effective-mass form factor

$$\begin{aligned}f_q(\boldsymbol{r}) =& 1 + \frac{2m}{\hbar^2}\left\{\frac{1}{4}\left[t_1\left(1+\frac{1}{2}x_1\right) + t_2\left(1+\frac{1}{2}x_2\right)\right]\rho(\boldsymbol{r})\right.\\ &\left. + \frac{1}{4}\left[t_2\left(x_2+\frac{1}{2}\right) - t_1\left(x_1+\frac{1}{2}\right)\right]\rho_q(\boldsymbol{r})\right\}\end{aligned} \tag{5}$$

and the spin-orbit density is expressed as:

$$\boldsymbol{J}_q = -\frac{1}{2}W_0\left(\frac{2m}{\hbar^2}\right)\frac{1}{f_q}\rho_q\nabla\rho_q. \tag{6}$$

The Coulomb energy density is a functional of proton density. Here we consider the contributions of the direct term and exchange term:

$$\mathcal{H}_{\rm Coul}(\boldsymbol{r}) = \frac{e^2}{2}\rho_p(\boldsymbol{r})\int\frac{\rho_p(\boldsymbol{r}')}{|\boldsymbol{r}-\boldsymbol{r}'|}\mathrm{d}\boldsymbol{r}' - \frac{3e^2}{4}\left(\frac{3}{\pi}\right)^{1/3}[\rho_p(\boldsymbol{r})]^{4/3}. \tag{7}$$

From eqs. (1)–(7), one can see that the total energy of a nucleus can be expressed as a functional of nuclear density and its gradients.

In the semi-classical ETF2 approach, the ground state deformations of deformed nuclei can not be accurately described due to the neglecting of the microscopic shell and pairing effects. However, based on the restricted density variational method together with the form of Woods-Saxon distribution:

$$\rho_q(\boldsymbol{r}) = \frac{\rho_0^{(q)}}{1+\exp\left[\frac{r-\mathcal{R}_q(\theta)}{a_q}\right]}, \tag{8}$$

for describing the density of an axially deformed nucleus, one can calculate the "macroscopic" part of the binding energy $\tilde{E}$ of a nucleus as a function of quadrupole deformation β_2. $\rho_0^{(q)}$ and a_q denote the central density and the surface diffuseness of nuclei, respectively. $\mathcal{R}_q$ defines the distance from the origin of the coordinate system to the point on the nuclear surface

$$\mathcal{R}_q(\theta) = R_q\,[1+\beta_2 Y_{20}(\theta)]. \tag{9}$$

The central density $\rho_0^{(q)}$ is determined from the conservation of particle number. At a given nuclear quadrapole deformation β_2, one can obtain the minimal energy $\tilde{E}(\beta_2)$ of the nuclear system since the total energy is expressed as a function of density and its gradients under the ETF2 approximation, by using the optimization algorithm [20] and varying the four variables R_p, a_p, R_n, a_n for the description of the proton and neutron density distributions.

To test the ETF2 approach, we study the root-mean-square (rms) charge radii and deformation energies of nuclei with this approach. In Table 1 we list the calculated rms charge radii of some spherical nuclei with the ETF2 approach by adopting the parameters set SkM*. We find that the deviations from the experimental data are generally smaller than 0.03 fm for these nuclei, which is comparable with the rms

error (0.028 fm) of the Hartree-Fock-Bogoliubov (HFB27) model [23]. In addition, the deformation energies, defined as the difference in energy of a nucleus between its spherical and equilibrium shapes, for isotopes of Uranium are also investigated with the ETF2 approach. To describe the ground state deformations of nuclei in this semi-classical model, the Strutinsky shell corrections from the universal parameterization [24] of deformed Woods-Saxon potential are added to the macroscopic energy $\tilde{E}$. In Figure 1, we show the calculated deformation energies for the isotopes of Uranium. The solid curve and squares denote the results of HFB27 and WS* [25] model, respectively. One sees that the results of ETF2 approach (solid circles) are comparable with those from the HFB27 and WS* mass models. These tests indicate that the semi-classical ETF2 approach together with the Skyrme energy-density functional is appropriate for the description of nuclear deformation energies.

3 Symmetry energy coefficients of finite nuclei

In this section, we first investigate the symmetry energy coefficient $a_{\rm sym}$ in the liquid drop mass formula at spherical shapes as a function of nuclear mass number, based on the semi-classical ETF2 approach. Then, the macroscopic energy of a deformed nuclear system is studied with the ETF2 approach and the deformation dependence of $a_{\rm sym}$ is also investigated.

Figure 2 shows the calculated Skyrme energy per particle $E_{\rm Sky}/A = \frac{1}{A}\int \mathcal{H}_{\rm Sky}\,{\rm d}\boldsymbol{r}$ as a function of isospin asymmetry for nuclei with $A = 100$. Here, the Coulomb interaction which

Table 1 Nuclear root-mean-square charge radii of some nuclei (in fm) from the Skyrme energy density functional plus the ETF2 approach by using the parameters set SkM*. The experimental data are taken from ref. [26]

Nucleus	^{48}Ca	^{64}Ni	^{90}Zr	^{116}Sn	^{144}Sm	^{208}Pb
SkM*	3.51	3.84	4.27	4.61	4.94	5.53
Experiment	3.48	3.86	4.27	4.63	4.95	5.50

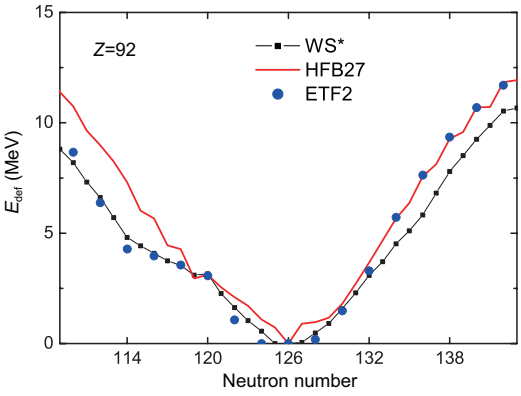

Figure 1 (Color online) Deformation energies of some isotopes of Uranium. The solid curve, squares and circles denote the results of HFB27, WS* [25], and ETF2 approach, respectively.

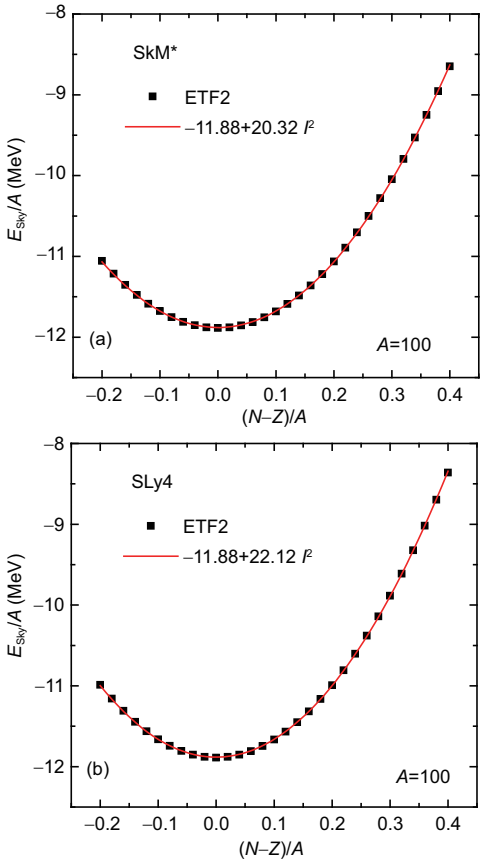

Figure 2 (Color online) Skyrme energy per particle as a function of isospin asymmetry $I = (N - Z)/A$ for nuclei with $A = 100$. (a) The results with the Skyrme force SkM*. (b) The results with SLy4. The Coulomb interaction is removed in the calculations.

can influence the density distributions of nuclei has been ignored in order to obtain the information of symmetry energy as clean as possible. In Figure 2, we set $\beta_2 = 0$ in the calculations. The solid squares denote the calculated results with the Skyrme energy density functional approach. According to the Bethe-Weizsäcker mass formula, the energy per particle of a nucleus subtracting the contribution of the Coulomb energy can be expressed as a function of mass number A and isospin asymmetry $I = (N - Z)/A$:

$$(E - E_{\rm c})/A = a_{\rm v} + a_{\rm s}A^{-1/3} + a_{\rm sym}I^2, \tag{10}$$

where $a_{\rm v}$, $a_{\rm s}$ denote the coefficients of the volume and the surface term, respectively. The parabolic law of the binding energies of nuclei is due to the isospin symmetry in nuclear physics. In the realistic nuclear system, the dependence of the asymmetry term is more complicated than the I^2 term. To give a qualitative view of the effects of nuclear deformations, we adopt the quadratic term for the description of the isospin asymmetry term. The coefficient $a_{\rm sym}$ of the quadratic term for the isospin asymmetry is the symmetry energy coefficient. The solid curves in Figure 2 denote the results from two-parameter parabola fitting to the

squares. The curvature of the solid curve represents the corresponding symmetry energy coefficient $a_{\rm sym}$ of finite nuclei with mass number A. The extracted symmetry energy coefficients for nuclei with A = 40, 100, 150, 208 are shown in Figure 3. With these four isobaric-chains, we can test the model for the description of the mass-dependence of $a_{\rm sym}$. The squares and stars denote the results with the parameter set SkM* and SLy4, respectively. Here, the nuclear deformations have not yet been taken into account. The values of $a_{\rm sym}(A)$ obtained in this approach are close to the results of ref. [15] in which the symmetry energy coefficients are extracted from the measured massed together with the formula $a_{\rm sym}(A) = S_0(1+\kappa A^{-1/3})^{-1}$ [27] for describing the mass-dependence. Here, S_0 is the volume symmetry energy coefficient of the nuclei (i.e. the nuclear symmetry energy at normal density) and κ is the ratio of the surface-symmetry coefficient to the volume-symmetry coefficient. The shades represent the uncertainty of the extracted symmetry energy coefficients [15]. From Figure 3, one can see that the results from the formula $a_{\rm sym}(A) = 31.1(1 + 2.31A^{-1/3})^{-1}$ are larger than those from SkM* and smaller than those from SLy4, because the corresponding values of S_0 are 30.0 and 32.0 MeV for SkM* and SLy4, respectively [28], and S_0 = 31.1 MeV for the solid curve. Here, we would like to state that the Coulomb energy term (see eq. (7)) is not involved in the calculation of the density distributions and the corresponding macroscopic energy $\tilde{E}$ of a nucleus. Considering the isospin dependence of the surface diffuseness obtained in the ETF2 approach, the Coulomb energy from the ETF2 approach could not be simply written as $a_c Z^2/A^{1/3}$ which is assumed for extracting the symmetry energy coefficient $a_{\rm sym}$ in ref. [15].

Now we come to the cases for deformed nuclei. With the same approach, the macroscopic energy $\tilde{E}$ of a nucleus with a certain quadrapole deformation β_2 can be calculated. Figure 4 shows the values of $E_{\rm Sky}/A$ as a function of isospin asymmetry for a series of nuclei with A = 100 under given nuclear quadrupole deformations. One sees that $E_{\rm Sky}/A$ changes with nuclear deformations, which could be due to the influence of surface-symmetry term and nuclear surface diffuseness. Similar to the spherical cases, the symmetry energy coefficients $a_{\rm sym}$ in the liquid drop formula can also be extracted for the deformed nuclei. We show in Figure 5 the symmetry energy coefficients of nuclei as a function of quadrupole deformation with SkM* and SLy4. The squares, circles, triangles and crosses denote the results for the isobaric nuclei with A = 40, 100, 150, 208, respectively. One sees that symmetry energy coefficients decrease with the increase of $|\beta_2|$. The large ground state deformations for some nuclei can cause the change of the symmetry energy coefficients by about 0.5 MeV. Therefore, the influence of nuclear deformations should be further considered if one wants to determine the symmetry energy coefficients more precisely from the masses.

Here, the curvature $\kappa_\beta = \frac{\partial^2 a_{\rm sym}}{\partial \beta_2^2}|_{\beta_2=0}$ of the symmetry energy coefficients in Figure 5 is simultaneously studied. Figure 6 shows the curvature of the symmetry energy coefficient as a function of mass number. The squares and stars denote the results of SkM* and SLy4, respectively. From Figure 6,

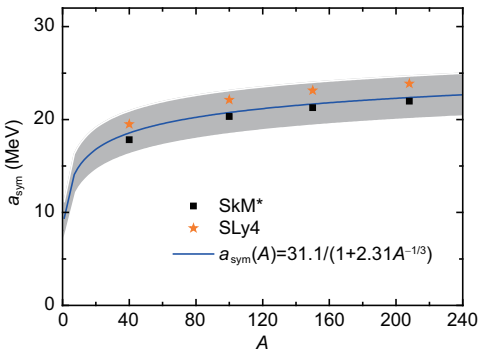

Figure 3 (Color online) Symmetry energy coefficients of nuclei as a function of mass number. The solid curve denotes the results of $a_{\rm sym}(A) = S_0(1 + \kappa A^{-1/3})^{-1}$ with S_0 = 31.1 MeV and κ = 2.31 which is taken from ref. [15]. The squares and stars denote the results with SkM* and SLy4, respectively.

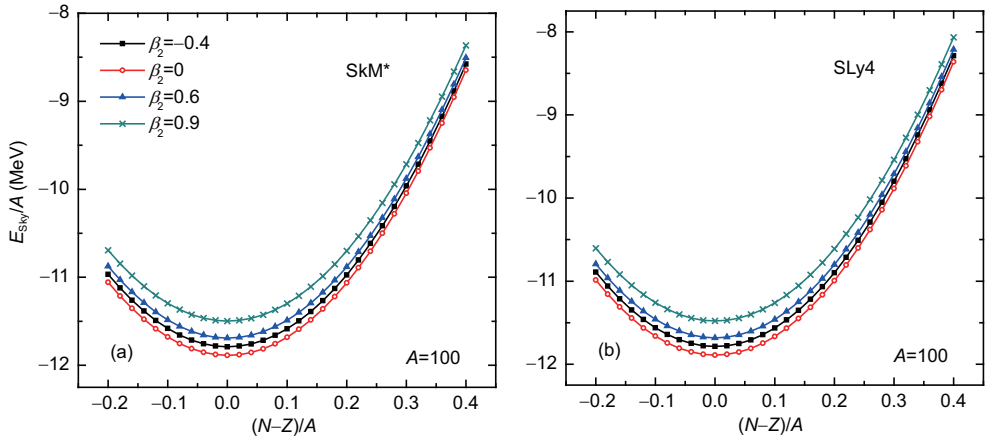

Figure 4 (Color online) The same as Figure 2, but with nuclear deformations β_2 = −0.4, 0, 0.6, 0.9.

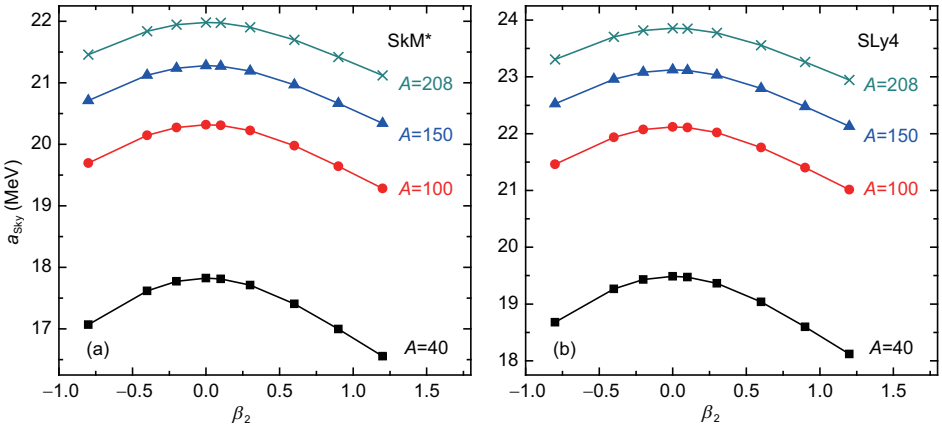

Figure 5 (Color online) Symmetry energy coefficients of nuclei as a function of quadrupole deformation.

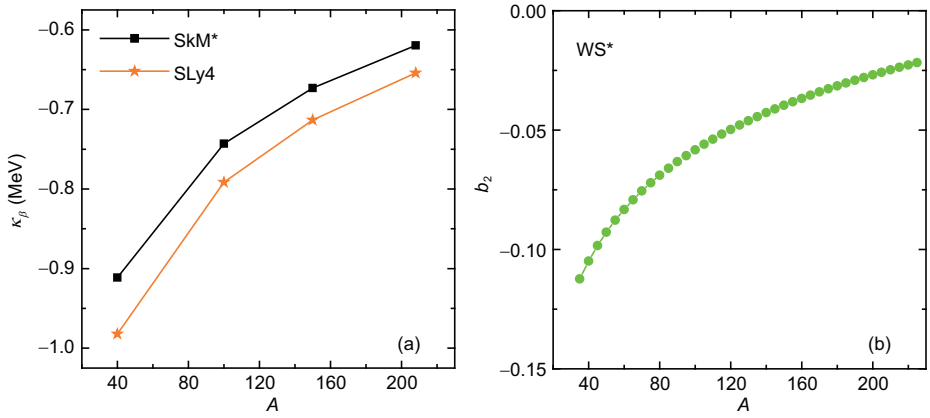

Figure 6 (Color online) (a) Curvature κ_β of the symmetry energy coefficients as a function of mass number. (b) Curvature of the parabola b_2 in the WS mass formula [25] for describing the deformation energies of nuclei.

one finds that the absolute value of κ_β decreases with the mass number, which is similar to the trend of the coefficient b_2 (see Figure 6(b)) of the nuclear deformation energy in the Weizsäcker-Skyrme mass formula [25, 29]. The influence of the quadrupole deformations on the symmetry energy coefficients gradually decreases with the increase of nuclear size. b_2 in Figure 6(b) denotes the (quadrupole) deformation energy coefficient which has a relationship with nuclear surface of finite nuclei and is therefore related to the surface-symmetry energy of nuclei.

To understand the deformation dependence of the symmetry energy coefficient, we further study the influence of nuclear surface diffuseness on $a_{\rm sym}$. In Figure 7(a), we show the calculated surface diffuseness of neutrons and protons for the isobaric chain $A = 100$ at spherical cases. Here, the Skyrme force SkM* is adopted. The open and solid circles denote the results for protons and neutrons, respectively. One sees that the isospin dependence of the surface diffuseness is evident. For neutron-rich nuclei, the symmetry potential will "push" the extra-neutrons to the very low density region [30]. If setting the surface diffuseness $a_n = a_p = 0.4$ fm in the calculations, we find that the values of $a_{\rm sym}$ slightly increase and the deformation dependence of the symmetry energy coefficient $a_{\rm sym}$ becomes weak (see Figure 7(b)). It indicates that the isospin dependence of the difference between the proton and neutron diffuseness plays a key role for the deformation dependence of the symmetry energy coefficient of finite nuclei.

4 Summary

In summary, by using the Skyrme energy density functional plus the extended Thomas-Fermi (ETF2) approximation, the symmetry energy coefficients of nuclei have been studied with the restricted density variational method. Considering nuclear quadrupole deformations in the calculations, we find that the calculated symmetry energy coefficient depends on not only the mass number A but also the nuclear deformations. The large deformations of nuclei can cause the change of symmetry energy coefficient by about 0.5 MeV. In the traditional liquid drop model, it is usually thought that only the surface energy and Coulomb energy terms are dependent on nuclear deformations. From the microscopic Skyrme energy density functional plus the ETF2 calculations, it is found that the isospin dependence of the difference between the proton and neutron diffuseness plays a key role for the deformation

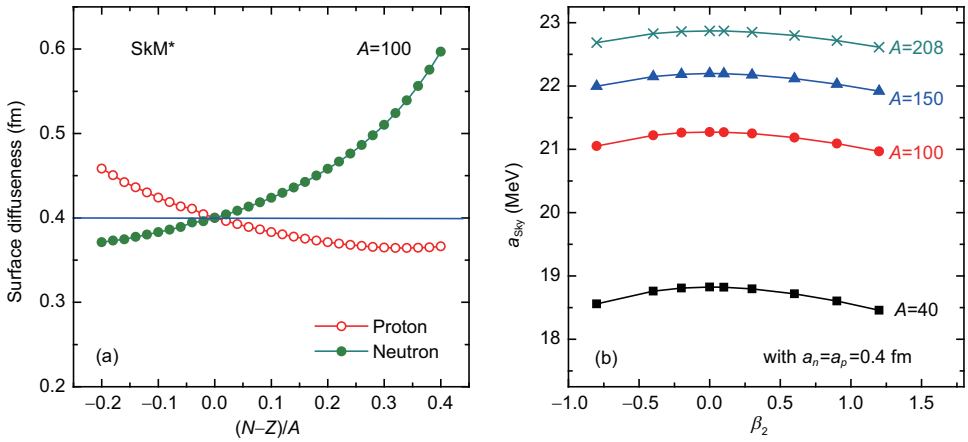

Figure 7 (Color online) (a) Nuclear surface diffuseness for nuclei with $A = 100$. (b) The same as Figure 5, but setting the surface diffuseness $a_p = a_n = 0.4$ fm in the calculations.

dependence of the symmetry energy coefficient of finite nuclei. These investigations are not only important for the study of symmetry energy, but also for the improvement of nuclear mass models.

This work was supported by the National Natural Science Foundation of China (Grants Nos. 11275052, 11365005 and 11422548).

1 Gandolfi S, Carlson J, Reddy S, et al. The equation of state of neutron matter, symmetry energy, and neutron star structure. Eur Phys J A, 2014, 50: 10
2 Zhang Y X, Danielewicz P, Famiano M, et al. The influence of cluster emission and the symmetry energy on neutron-proton spectral double ratios. Phys Lett B, 2008, 664: 145
3 Tsang M B, Zhang Y X, Danielewicz P, et al. Constraints on the density dependence of the symmetry energy. Phys Rev Lett, 2009, 102: 122701
4 Li B A, Chen L W, Ko C M. Recent progress and new challenges in isospin physics with heavy-ion reactions. Phys Rep, 2008, 464: 113–281
5 Li B A, Das C B, Das Gupta S, et al. Momentum dependence of the symmetry potential and nuclear reactions induced by neutron rich nuclei at RIA. Phys Rev C, 2004, 69: 011603
6 Chen L W, Ko C M, Li B A. Determination of the stiffness of the nuclear symmetry energy from isospin diffusion. Phys Rev Lett, 2005, 94: 032701
7 Shetty D V, Yennello S J, Souliotis G A. Density dependence of the symmetry energy and the nuclear equation of state: A dynamical and statistical model perspective. Phys Rev C, 2007, 76: 024606
8 Botvina A S, Lozhkin O V, Trautmann W. Isoscaling in light-ion induced reactions and its statistical interpretation. Phys Rev C, 2002, 65: 044610
9 Centelles M, Roca-Maza X, Vinas X, et al. Nuclear symmetry energy probed by neutron skin thickness of nuclei. Phys Rev Lett, 2009, 102: 122502
10 Steiner A W, Gandolfi S. Connecting neutron star observations to three-body forces in neutron matter and to the nuclear symmetry energy. Phys Rev Lett, 2012, 108: 081102
11 Steiner A W, Prakash M, Lattimer J M, et al. Isospin asymmetry in nuclei and neutron stars. Phys Rep, 2005, 411: 325–375
12 Dong J, Zuo W, Scheid W. Correlation between α-decay energies of superheavy nuclei involving the effects of symmetry energy. Phys Rev Lett, 2011, 107: 012501
13 Wang N, Ou L, Liu M. Nuclear symmetry energy from the Fermi-energy difference in nuclei. Phys Rev C, 2013, 87: 034327
14 Wang N, Li T. Shell and isospin effects in nuclear charge radii. Phys Rev C, 2013, 88: 011301(R)
15 Liu M, Wang N, Li Z X, et al. Nuclear symmetry energy at subnormal densities from measured nuclear masses. Phys Rev C, 2010, 82: 064306
16 Audi G, Wapstra A H, Thibault C. The AME 2003 atomic mass evaluation (II). Tables, graphs and references. Nucl Phys A, 2003, 729: 337–676
17 Vautherin D, Brink D M. Hartree-fock calculations with skyrme's interaction. I. Spherical nuclei. Phys Rev C, 1972, 5: 626
18 Bartel J, Bencheikh K. Nuclear mean fields through self-consistent semiclassical calculations. Eur Phys J, 2002, 14: 179–190
19 Brack M, Guet C, Hakanson H B. Selfconsistent semiclassical description of average nuclear properties ł a link between microscopic and macroscopic models. Phys Rep, 1985, 123: 275–364
20 Liu M, Wang N, Li Z, et al. Applications of Skyrme energy-density functional to fusion reactions spanning the fusion barriers. Nucl Phys A, 2006, 768: 80–98
21 Bartel J, Quentin P, Brack M, et al. Towards a better parametrisation of Skyrme-like effective forces: A critical study of the SkM force. Nucl Phys A, 1982, 386: 79–100
22 Chabanat E, Bonche P, Haensel P, et al. A Skyrme parametrization from subnuclear to neutron star densities Part II. Nuclei far from stabilities. Nucl Phys A, 1998, 635: 231–256
23 Goriely S, Chamel N, Pearson J M. Hartree-Fock-Bogoliubov nuclear mass model with 0.50 MeV accuracy based on standard forms of Skyrme and pairing functionals. Phys Rev C, 2013, 88: 061302(R)
24 Cwoik S, Dudek J, Nazarewicz W, et al. Single-particle energies, wave functions, quadrupole moments and g-factors in an axially deformed woods-saxon potential with applications to the two-centre-type nuclear problems. Comp Phys Comm, 1987, 46: 379–399
25 Wang N, Liang Z, Liu M, et al. Mirror nuclei constraint in nuclear mass formula. Phys Rev C, 2010, 82: 044304
26 Angeli I, Marinova K P, Data At, et al. Table of experimental nuclear ground state charge radii: An update. Data Tables, 2013, 99: 69–95
27 Danielewicz P, Lee J. Symmetry energy I: Semi-infinite matter. Nucl Phys A, 2009, 818: 36–96
28 Dutra M, Lourenço O, Sá Martins J S, et al. Skyrme interaction and nuclear matter constraints. Phys Rev C, 2012, 85: 035201
29 Wang N, Liu M, Wu X Z. Modification of nuclear mass formula by considering isospin effects. Phys Rev C, 2010, 81: 044322
30 Wang N, Liu M, Wu X Z, et al. Surface diffuseness correction in global mass formula. Phys Lett B, 2014, 734: 215